

An Architecture for a Wavelength-Interchanging Cross-Connect Utilizing Parametric Wavelength Converters

N. Antoniadou, *Member, IEEE*, S. J. B. Yoo, *Senior Member, IEEE, Member, OSA*, Krishna Bala, Georgios Ellinas, *Member, IEEE*, and Thomas E. Stern, *Life Fellow, IEEE*

Abstract— This paper proposes an architecture for a wavelength-interchanging cross-connect (WIXC) that can be used as a switching node of strictly transparent and scalable networks with all-optical routing and all-optical wavelength conversion capabilities. This architecture utilizes all-optical parametric wavelength converters based on difference-frequency-generation (DFG) or four-wave mixing (FWM), although this work focuses only on the implementation using Difference-Frequency-Generation wavelength converters. The proposed WIXC architecture exploits the unique wavelength mapping properties of parametric wavelength converters: mirror image mapping and simultaneous multichannel wavelength conversion. The derivation of this architecture involves application of a Space/Wavelength transformation to the classical Benes switch fabric. The connection setup for the resulting architecture follows the well established looping algorithm, and the architecture is scalable in both the ports and the wavelengths. The scaling occurs in an orderly fashion, which allows modular upgrades of WIXC's for cost-effective evolution of the networks. The unique properties of the parametric wavelength converter including transparent and multichannel conversion capabilities result in a WIXC architecture that requires fewer wavelength converters while maintaining scalability and transparency.

Index Terms— Architecture, optical networks, transparency, wavelength conversion, wavelength division multiplexing (WDM), wavelength interchange cross-connect (WIXC), wavelength selective cross-connect (WSXC).

I. INTRODUCTION

IN recent years, significant research efforts have been devoted to the design of high-capacity, flexible, cost-effective, reliable, transparent, and scalable multiwavelength optical networks [1], [2]. Dense wavelength division multiplexing (DWDM) point-to-point transmission is emerging as the key technology solution that will help increase capacity and realize national scale networks. The DWDM point-to-point systems

are starting to give way to purely optical networking connections where nodes can perform all-optical routing, opening the way for scalable and transparent optical networks.

A truly transparent network acts as a transparent "ether" through which one can launch a signal of any type, unspecified bit rate, modulation format and phase, and nothing will interfere with it until it reaches the receiver [3]. Moreover, transparent networks allow all-optical signals to propagate in an express fashion through the network without costly and sometimes unnecessary opto-electronic conversions.

Scalability implies that the network can grow gracefully in size, capacity, number of nodes, and hence, in number of users. A truly scalable network will ideally have the capability of expanding the number of nodes without increasing the number of wavelengths available for optical connections. This will require wavelength reuse and might benefit from wavelength conversion or interchange. Wavelength reuse is required because the number of active optical connections in a network typically grows faster than the number of links and nodes. Wavelength interchange might help circumvent the limitation in the reach of an optical path imposed by the constraint of wavelength continuity. To establish an optical connection along a path consisting of several links in a WDM network, a wavelength must be free on each of the links of the path. Without wavelength interchange at the network nodes, wavelength continuity requires that the free wavelength must be the same on each link. This requirement is often difficult to satisfy in heavily loaded networks and on paths composed of a large number of optical hops, thereby creating significant "blocking" of long connections in those networks. By introducing wavelength interchange at the network nodes, the wavelength continuity constraint is removed, so that a connection can be activated as long as there is at least one free wavelength on each link on the path, without requiring the free wavelength to be the same. Thus, wavelength interchange effectively extends the reach of these connections. If this wavelength interchange is performed by all-optical strictly transparent devices, transparent and scalable optical networks can be achieved.

Wavelength conversion is usually performed inside the complex optical cross-connects called wavelength interchange cross-connects (WIXC's) either before or after the switching fabrics. A WIXC is a network element that accepts multiwavelength signals from a transport facility at its input

Manuscript received May 28, 1998; revised December 4, 1998. This work was supported in part by DARPA under the MONET program.

N. Antoniadou was with the Center for Telecommunications Research, Department of Electrical Engineering, Columbia University, New York, NY 10027 USA. He is now with Corning Inc., Somerset, NJ 08873 USA.

S. J. B. Yoo was with Bellcore, Red Bank, NJ 07701 USA. He is now with the Department of Electrical and Computer Engineering, University of California, Davis 95616 USA.

K. Bala is with Tellium Inc., Edison, NJ 08837 USA.

G. Ellinas is with Telcordia (formerly Bellcore), Red Bank, NJ 07701 USA.

T. E. Stern is with the Department of Electrical Engineering, Columbia University, New York, NY 10027 USA.

Publisher Item Identifier S 0733-8724(99)05528-0.

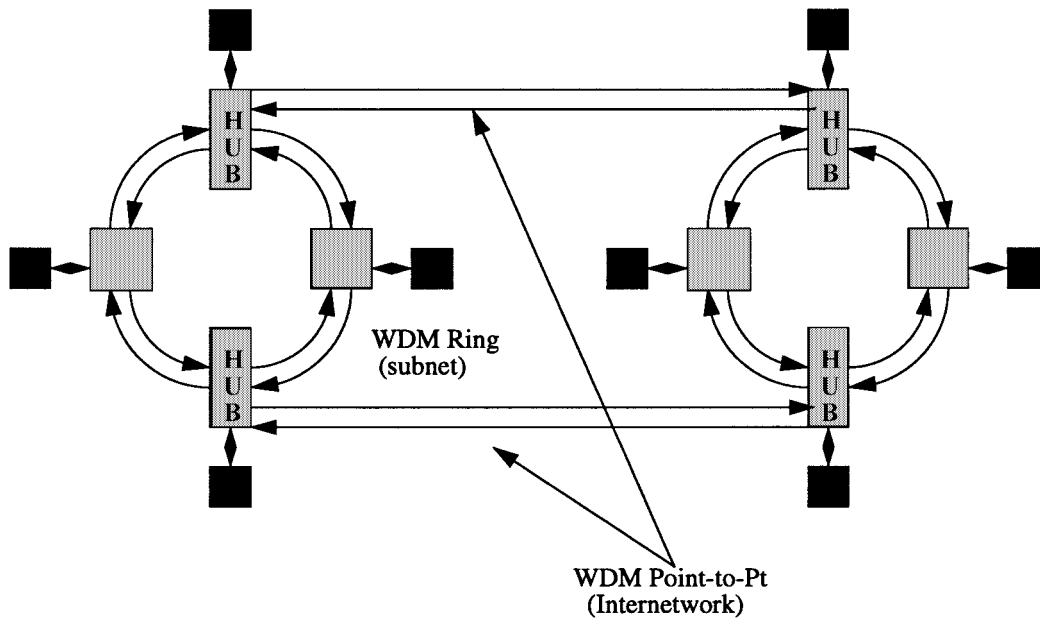


Fig. 1. WDM networks where wavelength-interchanging cross-connects (WIXC) are utilized. The two WDM ring subnetworks are connected to each other by four HUB's which include WIXC's.

ports and routes these signals using wavelength interchange (when necessary) to its output ports. A nonblocking WIXC provides cross-connection and wavelength conversion of any wavelength at any input port to any wavelength at any output port. While networks with full wavelength conversion can achieve higher capacity than networks without it, the full wavelength conversion at every node requires populating it with WIXC's rather than the simpler wavelength selective cross-connects (WSXC's) that do not have the wavelength interchange feature [4]. A common approach is to use the WIXC's at a small number of sparsely dispersed locations in the network, thus obtaining the full-performance benefits of the technology [5]. Fig. 1 shows an example of two rings interconnected by four WIXC's. A common network control permits their dynamic rearrangability.

A number of research consortia including multiwavelength optical networking (MONET) have proposed and implemented WSXC's for wavelength routing and reuse in the network [4]. WDM networks that use WIXC's have also been proposed [6]–[9]. Fig. 2 shows a WIXC architecture widely proposed in the literature [10]. This architecture has a space-switch fabric followed by an array of wavelength converters. The wavelength converters must have variable-input to fixed-output mapping properties, thus limiting the transparency of the resulting WIXC. Future upgrades of the above WIXC architecture by increasing the number of wavelengths or ports will require major changes in the size of the switching fabric, the number of (de)multiplexers (MUX's/DMUX's) and more importantly the number of all-optical wavelength converters thus imposing constraints on the scalability of the architecture.

In this paper, we propose an architecture for a WIXC that preserves network transparency and provides network scalability. The operation of the proposed WIXC architecture is based on the use of parametric wavelength converters [11] and stems from the classical Benes switch fabric. The architecture

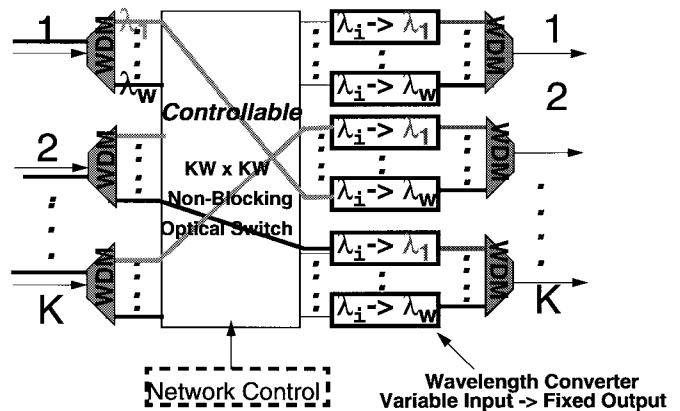


Fig. 2. Frequently proposed wavelength-interchange cross-connect architecture.

capitalizes on the unique mapping properties of parametric wavelength converters. These properties include simultaneous conversion of multiple wavelengths and a mirror-image mapping function for all the converted wavelengths. This architecture is valid for parametric processes such as difference frequency generation (DFG) and four-wave mixing (FWM). DFG is free from cross-mixing terms present in FWM and other higher order parametric processes. It also offers a method for effectively filtering unwanted wavelengths, while providing polarization-insensitive wavelength conversion [12]. For these reasons, we will discuss the proposed WIXC architecture in the context of DFG wavelength converters even though other parametric wavelength converters can, in principle, utilize the proposed WIXC architecture. The resulting architecture offers the scalability inherent in the Benes switch fabric (scalable in a recursive manner) with the strict transparency achieved by parametric wavelength conversion. These properties, as mentioned above, are especially attractive when future network upgrades with full interoperability are considered.

Section II introduces the DFG wavelength conversion and its main operating characteristics. Section III describes the basic $2 \times 2/2-\lambda$ WIXC architecture and how is derived based on the Space/Wavelength transformation, and Section IV generalizes the above architecture to any number of ports K and any number of wavelengths W . Section V discusses the routing algorithm for the proposed WIXC and Section VI gives a comparison of the number and types of wavelength converters and other components needed for different existing and proposed WIXC architectures. Some final thoughts and conclusions are presented in Section VII followed by the Appendix where the DFG converter types are described in more detail.

II. DFG WAVELENGTH CONVERTER

Transparency in all-optical networks provides a number of benefits not available in traditional networks. It facilitates interoperability and network evolution, while accommodating users of various signal formats and protocols. While there are obvious benefits of transparency, wavelength conversion is likely to be the first obstacle in realizing transparent WDM networks. The majority of available wavelength conversion methods, whether all-optical or optoelectronic, offer only limited transparency [13]. Only under controlled conditions, they are transparent to digital signals of various bit rates. They often are accompanied by noise from spontaneous emission background or electronic amplification. In contrast, parametric wavelength conversion processes such as DFG and FWM provide strictly transparent wavelength conversion without adding excess noise [13]. These are based on the nonlinear optical response of the medium when more than one wave is present. DFG is based on the second-order nonlinear effect and FWM is based on the third order nonlinearity [14].

Parametric wavelength conversion not only provides strict transparency but also possesses unique mapping properties. It offers mirror image mapping and converts multiple wavelengths simultaneously. Fig. 3 illustrates an example of the DFG wavelength converter. The DFG wavelength converter generates an output signal at wavelength λ'_i by mixing with an input signal at wavelength λ_i and a pump at wavelength λ_p according to the frequency mixing equation

$$\frac{1}{\lambda'_i} = \frac{1}{\lambda_p} - \frac{1}{\lambda_i}. \quad (1)$$

The parametric wavelength converter allows more than one input wavelength, in which case, each set of input and output wavelengths follows the same energy relation shown in (1). If four input wavelengths, λ_1 , λ_2 , λ_3 , and λ_4 , are equally spaced in frequency, the application of a pump wavelength at λ_p , where $(1/\lambda_p) = (1/\lambda_2) + (1/\lambda_3)$, will convert their output wavelengths to λ_4 , λ_3 , λ_2 , and λ_1 , respectively. Hence, the information carried on the input wavelengths is interchanged to the output wavelengths by a mirror image mapping relation between input and output wavelengths as though a mirror were placed at $2\lambda_p$ (between wavelengths λ_2 and λ_3). The two examples in Fig. 3 present multiple input wavelength conversion cases where information is interchanged amongst a set of wavelengths.

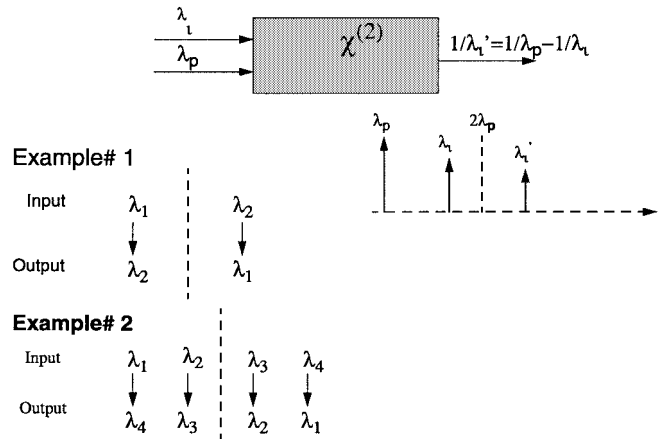


Fig. 3. Black box representation of the bulk wavelength conversion and mirror image mapping properties of a difference frequency generation wavelength converter.

The goal of this work is to utilize the multichannel, mirror-image mapping characteristics of parametric wavelength conversion for implementing a WIXC architecture, which serves as a foundation for realizing a strictly transparent WIXC. In principle, both FWM and DFG parametric wavelength conversion mechanisms possess mathematically identical multichannel, mirror-image mapping characteristics as discussed above. However, the following differences between the two physical mechanisms make application of FWM to the proposed WIXC architecture more difficult. First, FWM produces additional cross-mixing terms, which interfere with other multiple wavelength channels. On the other hand, the DFG wavelength converters accompany negligibly small (typically more than 60 dB below the signal level) cross-mixing terms rising from higher order effects like FWM. Second, there is no simple method to filter unwanted signals in FWM when multiple channels are present. This is especially true for FWM which involves the pump wavelength serving as the mirror plane in the same wavelength range as the signal wavelengths. The method discussed in [15] provides reasonably effective filtering, but not sufficient to suppress coherent cross-talk penalties. For DFG, there are several methods as reported in [12]. Thirdly, there is no known method to achieve polarization insensitive wavelength conversion by FWM utilizing a single pump wave. Recent results utilizing two orthogonally polarized pump waves achieved polarization independent wavelength conversion [16], but this method produces even larger number of cross-mixing terms. The DFG converter on the other hand exhibits polarization diversified operation and polarization-independent conversion efficiency [11], [12]. Based on the above observations we will consider only DFG parametric wavelength conversion hereafter. Recent experimental results in DFG wavelength conversion seem quite promising for WIXC applications. Fig. 4(a), shows the measured output spectra of the DFG wavelength converter for two-input wavelengths. Multiple wavelength conversion with no measurable cross-mixing term is demonstrated. Fig. 4(b) presents the measured conversion efficiency as a function of input wavelength for two input polarizations. As is expected from theory, the experiment demonstrates polarization

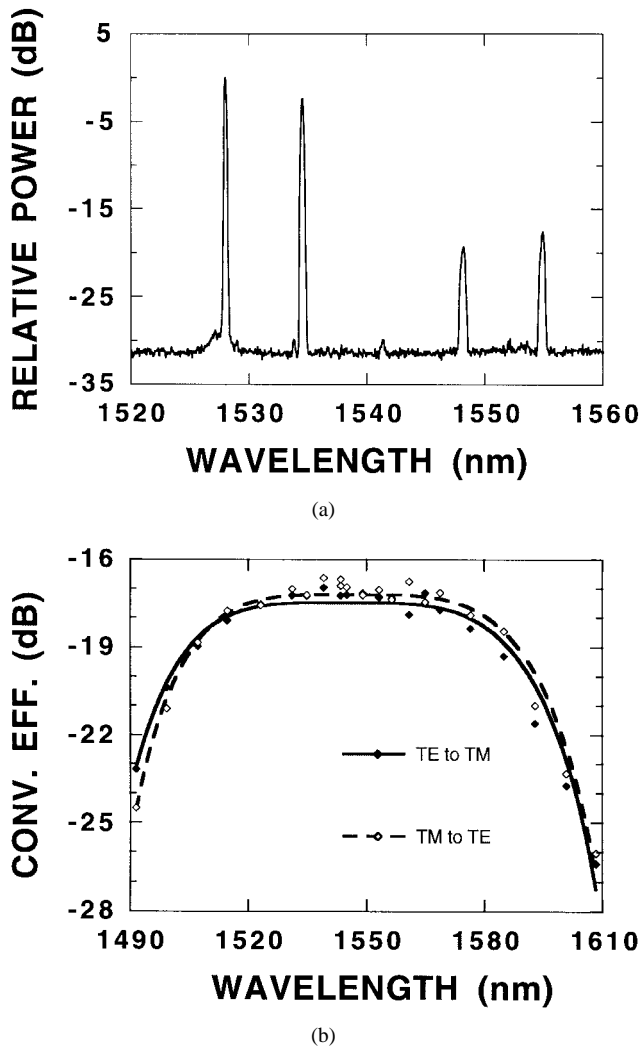


Fig. 4. (a) Measured output spectra of the wavelength converter. The 1532-nm wave (λ_1) and 1528 nm wave (λ_2) are the two-input signal waves and 1549 nm wave (λ'_1) and 1555 nm wave (λ'_2) are the resulting converted (idler) waves; (b) Measured conversion efficiency as a function of the input wavelength for the two-input signal polarization states. Both sets of data points are curve fit according to theory.

diversified wavelength conversion (transverse electric (TE) input to transverse magnetic (TM) output and vice versa) as well as polarization independent conversion efficiency (in terms of optical power) [11]. This figure also demonstrates an extremely broad conversion bandwidth of 90 nm. The conversion efficiency is -17 dB for a 65-mW pump power [11]. This is far below the theoretically calculated value of -4 dB for 100 mW pump power, however, the efficiency is expected to improve with reduction in optical loss in the fabricated device. Recently, there has been significant work on improving the performance and showing the viability of the DFG wavelength converter [17]. We now discuss in detail the proposed WIXC architecture.

III. PARAMETRIC WIXC ARCHITECTURE

The construction of an WIXC architecture built around the parametric wavelength converter involves utilization of its unique multichannel, mirror mapping property. We start

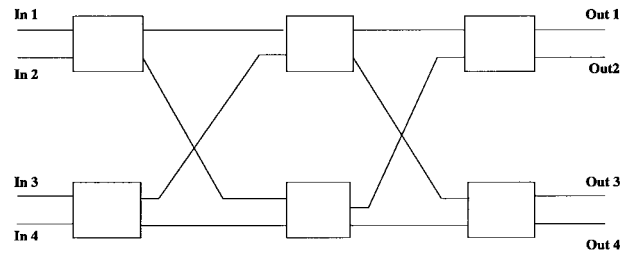


Fig. 5. A 4×4 Benes network.

from a classical Benes switch fabric [18] which has well known properties. Fig. 5 shows a 4×4 Benes network. Two steps are necessary for the construction of the proposed architecture. We apply a space/wavelength transformation proposed by Hunter and Thompson [19], which we refer to as the “Hunter–Thompson space/wavelength transformation.” Fig. 6(a) illustrates a $2 \times 2/2-\lambda$ WIXC which results from applying the “Hunter–Thompson Space/Wavelength transformation” to the Benes network of Fig. 5. This transformation essentially means relabeling, and twisting around the Benes interconnections. Foundation of this transformation lies in the earlier work on space/time transformation presented in Marcus’ seminal paper [20]. The design of Fig. 6(a) is equivalent to the Benes design and thus is rearrangeably nonblocking. This intermediate step architecture will be referred to as the “Twisted Benes” design. The label $\lambda_i^{P_j}$ stands for the signal of wavelength i and port j . The dotted line shown in Fig. 6(a) is the wavelength plane that separates the ports associated with λ_1 from the others associated with λ_2 . Signals crossing over this dotted line undergo wavelength conversion from one wavelength to another. Note that the crossover occurs symmetrically around the dotted line, which implies a wavelength conversion with mirror image mapping is suitable. The above presents only the theoretical “Twisted Benes” architecture resulting from the “Hunter–Thompson space/wavelength transformation.” Construction of the actual $2 \times 2/2-\lambda$ WIXC shown in Fig. 6(b) results from overlapping the upper and the lower half of the “Twisted Benes” architecture of Fig. 6(a) and inserting DFG wavelength converters at the crossing points. The boxes labeled W_c are wavelength converters translating λ_1 to λ_2 and λ_2 to λ_1 . The space switches in Fig. 6(b) differ from those in Figs. 5 and 6(a) in that each of them is a wavelength selective cross-connect (WSXC) configured to operate in the cross or bar state independently for every individual wavelength. These WSXC’s can be acoustooptic tunable filters (AOTF’s) [21], liquid-crystal switches [22], hybrid technology switches made of WDM MUX’s/DMUX’s [23], or any other wavelength selective switch design.

Fig. 7(a) illustrates the following set of sample connections:

$$\begin{aligned} \lambda_1^{P1} &\text{ to } \lambda_2^{P2} \\ \lambda_2^{P1} &\text{ to } \lambda_1^{P2} \\ \lambda_1^{P2} &\text{ to } \lambda_1^{P1} \\ \lambda_2^{P2} &\text{ to } \lambda_2^{P1}. \end{aligned}$$

The routing algorithm used for setting up this permutation

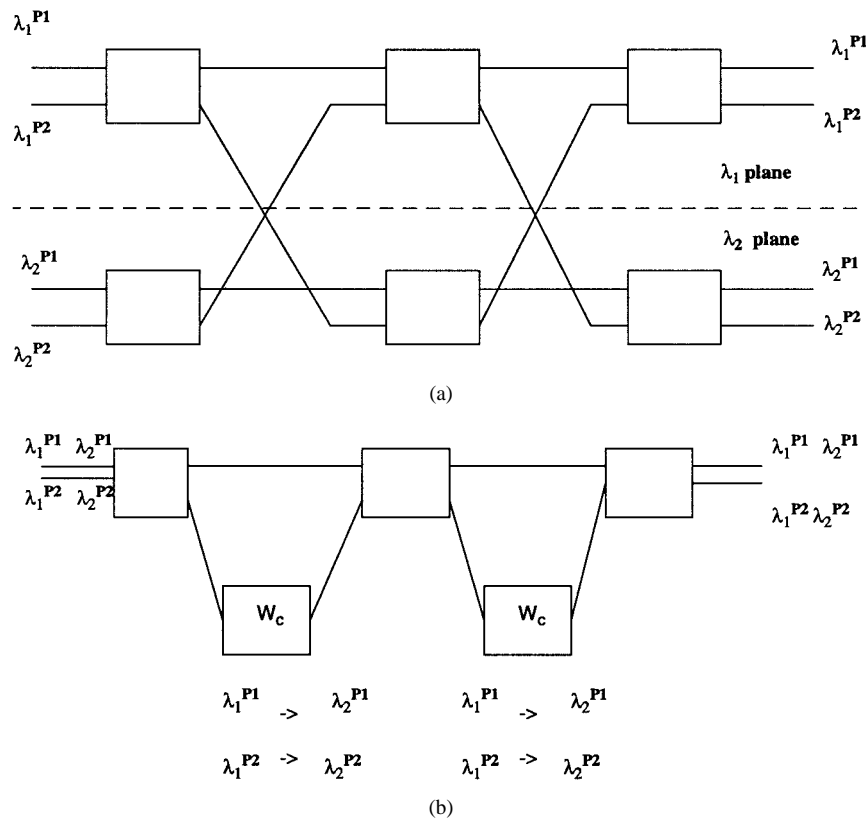


Fig. 6. Results from applying the “Hunter–Thompson Space/Wavelength transformation” on the 4×4 Benes architecture of Fig. 5. (a) The theoretical “Twisted Benes” design and (b) the actual $2 \times 2/2-\lambda$ WIXC architecture.

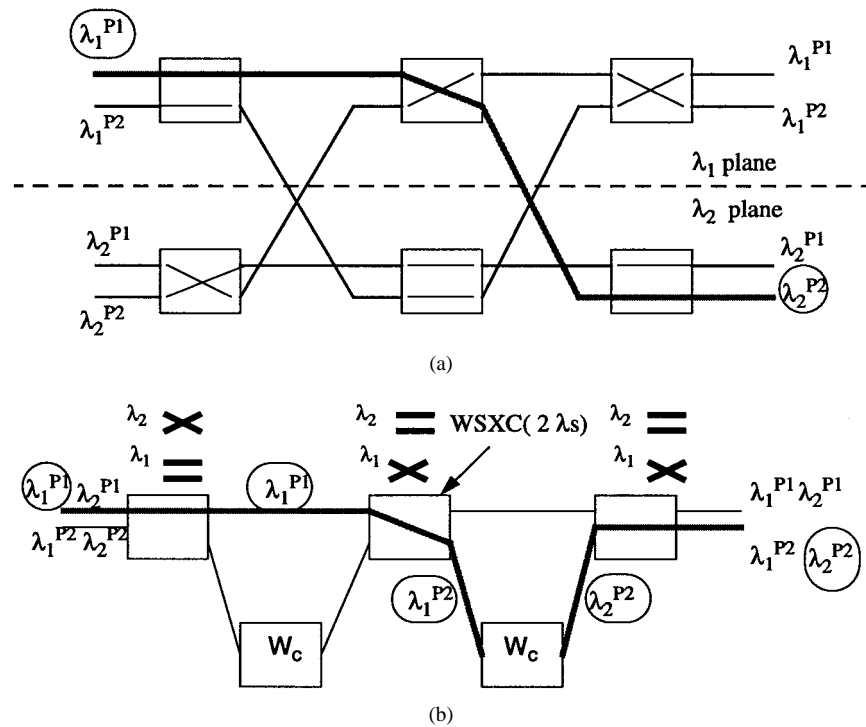


Fig. 7. (a) A 4×4 “Twisted Benes” with sample connection pattern; (b) $2 \times 2/2-\lambda$ WIXC implementation using DFG parametric wavelength converters.

can be obtained from [24] and will be discussed further in Section V. Fig. 7(b) shows the actual WIXC indicating the states of all the space switches which are obtained by simply

looking at the switch state of the corresponding wavelength plane in Fig. 7(a). The gray line traces one of the connections from λ_1^{P1} to λ_2^{P2} .

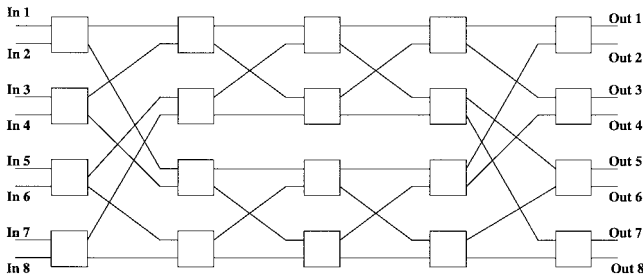


Fig. 8. An 8×8 Benes network.

IV. GENERALIZED PARAMETRIC WIXC ARCHITECTURES

The previous section dealt with a very specific WIXC architecture namely the $2 \times 2/2-\lambda$ architecture. In this section, we show that it is possible to expand to architectures of larger number of wavelengths and finally to architectures of arbitrary number of ports and wavelengths.

Fig. 8 shows an 8×8 Benes switch. Generalization of the “Twisted Benes” design and the parametric WIXC’s to larger number of ports and wavelengths requires twisting and relabeling of ports with some extra port adjustment in order to accommodate for the DFG wavelength converter’s mirror image property. For the above 8×8 Benes switch, twisting and relabeling of ports produces the switch fabric of Fig. 9(a). This shows a $2 \times 2/4-\lambda$ WIXC architecture where the ports have been labeled so as to create four virtual wavelength planes. The interstage connections between stages 1 to 2 and stages 4 to 5 are twisted in a manner such that it is possible to change between wavelength planes 1 and 4 and planes 2 and 3. The rest of the network stages are constructed recursively with twisted Benes subnetworks. Since this design has been derived from an 8×8 Benes switch, by twisting some of its ports, it remains to be proven that its rearrangeably nonblocking property remains intact. This will be done in Section V by referring to the Slepian and Duguid theorem that makes use of the recursive nature of the architecture. Section V will also deal with the routing algorithm used to establish the set of connections in this architecture. Fig. 9(a) includes the following set of sample connections:

$$\begin{aligned} &\lambda_1^{P1} \text{ to } \lambda_3^{P2} \\ &\lambda_1^{P2} \text{ to } \lambda_4^{P1} \\ &\lambda_2^{P1} \text{ to } \lambda_4^{P2} \\ &\lambda_2^{P2} \text{ to } \lambda_3^{P1} \\ &\lambda_3^{P1} \text{ to } \lambda_1^{P2} \\ &\lambda_3^{P2} \text{ to } \lambda_1^{P1} \\ &\lambda_4^{P1} \text{ to } \lambda_2^{P1} \\ &\lambda_4^{P2} \text{ to } \lambda_2^{P2}. \end{aligned}$$

Fig. 9(b) shows the corresponding $2 \times 2/4-\lambda$ actual WIXC implementation. In this figure, W_{sp}^{23} refers to a single-pumped DFG converter which is a standard mirror image wavelength converter, with the mirror placed between λ_2 and λ_3 . W_{dp}^{12+34} refers to a double-pumped DFG converter with two pumps: one pump for the λ_1 and λ_2 interchange (mirror between λ_1 and λ_2), and another pump for the λ_3 and λ_4 interchange

(mirror between λ_3 and λ_4). A single pump is needed for the wavelength conversion of λ_1 and λ_2 to λ_4 and λ_3 , respectively, whereas a double pump is used for the simultaneous conversions from λ_1 to λ_2 and λ_3 to λ_4 . The routing on the actual WIXC of Fig. 9(b) is based on the establishment of the random set of connections of Fig. 9(a) and is done by looking at the switch state of the corresponding wavelength plane of Fig. 9(a). The gray line in Fig. 9(a) and (b) traces a connection from λ_1^{P1} to λ_3^{P2} .

Fig. 10 shows another example of an expanded WIXC using a 16×16 input–output architecture. By appropriately labeling the ports we can achieve the actual $2 \times 2/8-\lambda$ WIXC as shown in Fig. 11. Again we have presented a random set of connections and a specific sample connection has been traced for illustration purposes. The actual WIXC of Fig. 11 includes seven serially connected eight-wavelength 2×2 switches and three types of wavelength interchangers, single-pumped, double-pumped and quad-pumped converters W_{qp} , serially connected between one set of ports of the switches. Although DFG wavelength converters with more than two pump waves are mathematically correct, there is no obvious method of filtering additional mappings of input signal wavelengths at this time. For instance, four pump waves will map each input signal wavelength to four converted wavelengths according to the four mapping functions dictated by the pump wavelengths. Only one of the converted waves will be utilized and there is no obvious method of filtering the three other waves. In addition to this issue, DFG wavelength converters with increased number of pump waves suffer lower conversion efficiency due to the tradeoff between the efficiency and the number of pump waves in the quasiphase matching scheme. As a result, DFG converters with more than two pumps are to be avoided in this paper although they are feasible for architecture considerations. Instead, the W_{qp} wavelength converter design of Fig. 11 can be implemented in two ways: either by using two double-pumped DFG converters or by using four single-pumped DFG converters (as discussed in the Appendix). Moreover, if the 16×16 “Twisted Benes” architecture of Fig. 10 is modified according to [25] to a rearrangeably nonblocking Linear Lightwave Benes design, the quad-pumped converters will no longer be needed. Instead, four broadcast stars can be used. Similar transformations can be used for smaller or larger “Twisted Benes” networks.

As should be apparent, higher order WIXC’s based on the “Twisted Benes” architecture can be constructed. In [26], a generalized K -port/ W -wavelength, wavelength-interchanging cross-connect is constructed resulting in a $KW \times KW$ WIXC as follows: first we create a $2 \times 2/W'-\lambda$ twisted Benes network with the correct labels, as described above. The number of ports and number of wavelengths are such that: $W' = KW/2$. Then group the outside 2×2 switches in groups of $K/2$ vertically contiguous 2×2 switches. Each group constitutes a $K \times K$ module consisting of $K/2$ 2×2 switches. The ports are then relabeled for the new $KW \times KW$ design. The ports of the first group are labeled as λ_1^{P1} to λ_1^{Pk} , the ports of the second group are labeled λ_2^{P1} to λ_2^{Pk} , etc., up to the ports of the W th group being labeled

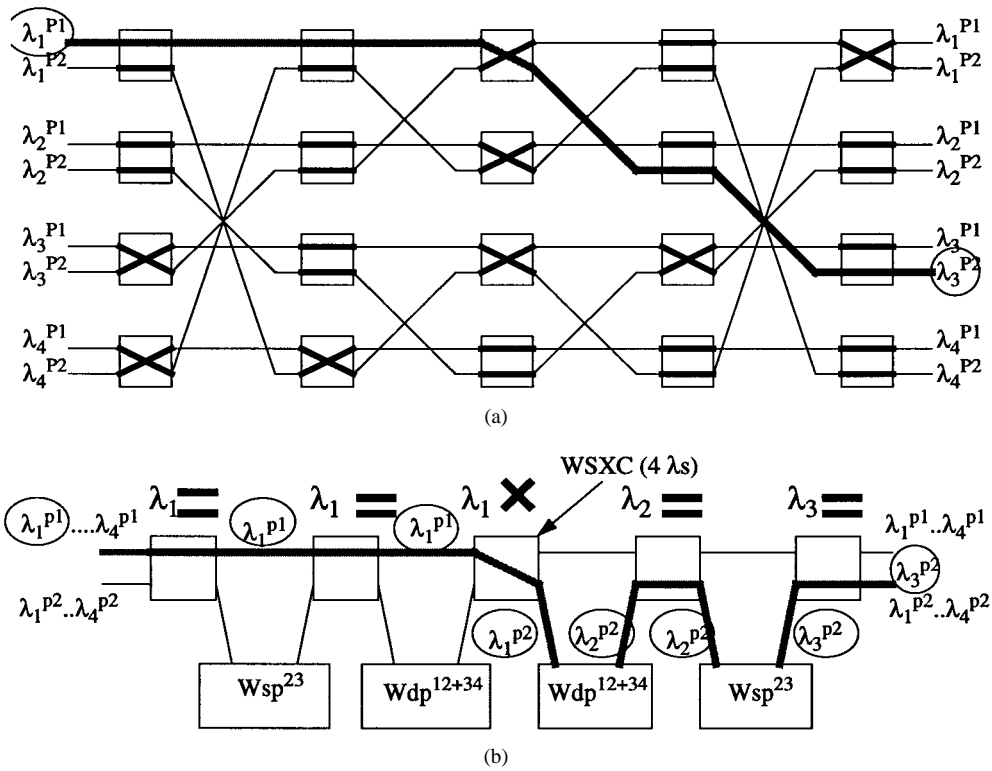


Fig. 9. (a) An 8×8 “Twisted Benes” with a random set of connections; (b) $2 \times 2/4-\lambda$ WIXC implementation using DFG parametric wavelength converters.

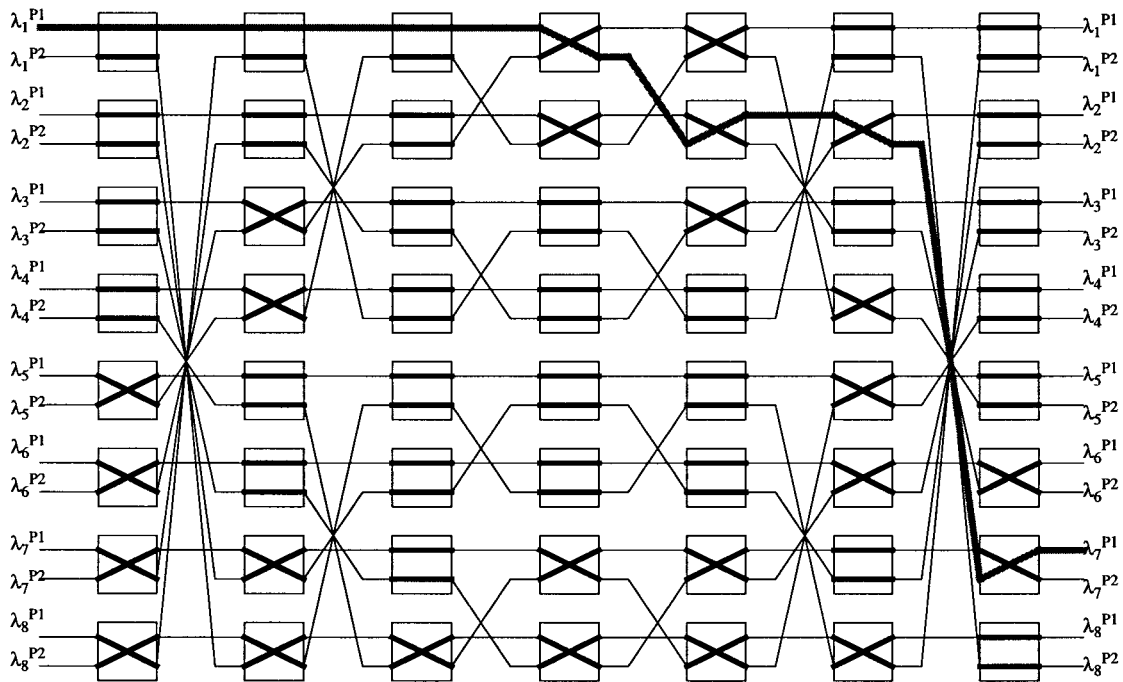


Fig. 10. A 16×16 “Twisted Benes” with a random set of connections.

as λ_w^{P1} to λ_w^{Pk} . The placement of the wavelength converters as well as the pumping wavelength and type is presented in detail in [26]. Fig. 12 shows the labeling for a $4 \times 4/2-\lambda$ WIXC that is created from the $2 \times 2/4-\lambda$ design of Fig. 9(a). In this case $K = 4$ and $W = 2$. Fig. 13 shows the actual WIXC implementation for the design of Fig. 12. It is obvious that the recursive nature of the architecture is maintained since

the grouping has no altering effect on the physical element connections (this is done only for port relabeling purposes).

As long as we have two input and two output ports, $K = 2$, the part count for both wavelength converters and wavelength-selective space switches increases slowly with the number of wavelengths and is given by $2\log(2W) - 2$ and $2\log(2W) - 1$ (\log is base 2), respectively. However, as the number W of

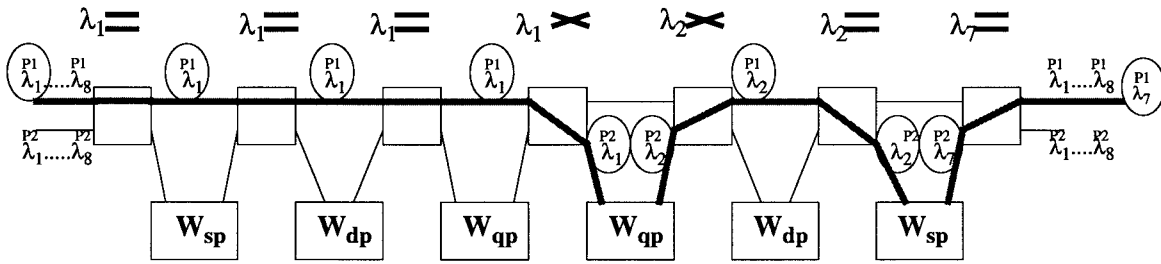


Fig. 11. A $2 \times 2/8-\lambda$ WIXC implementation using DFG parametric wavelength converters.

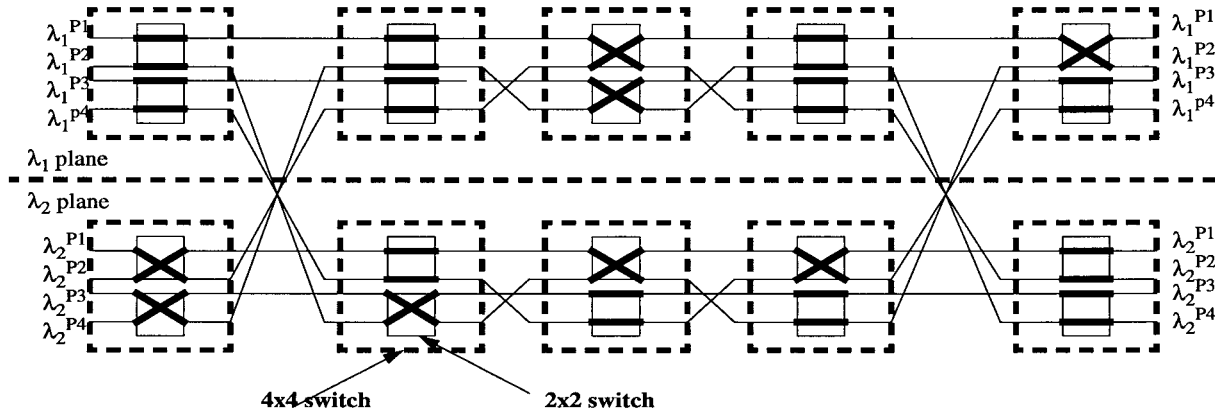


Fig. 12. Schematic view of the grouping and relabeling procedure for the 8×8 "Twisted Benes" of Fig. 9 that results in a $4 \times 4/2-\lambda$ architecture.

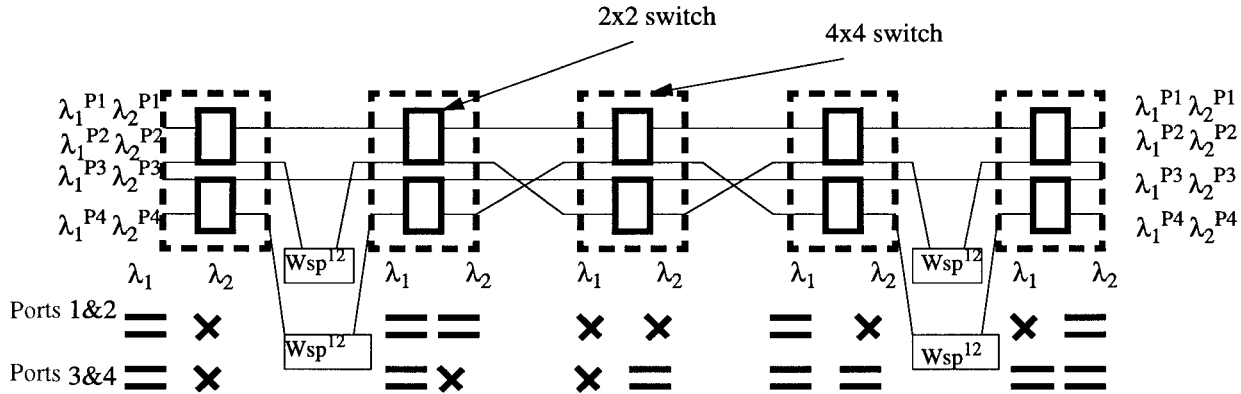


Fig. 13. A $4 \times 4/2-\lambda$ WIXC implementation using DFG parametric wavelength converters.

wavelengths increases ($W \geq 8$), at least one quad-pumped DFG wavelength converter is needed resulting in the previously mentioned difficulties. It is also difficult in this case to derive a general expression for the number of required wavelength converters. However, a more relevant part count for wavelength converters is the number of single-pumped or double-pumped wavelength converters. For example, for a $2 \times 2/8-\lambda$ WIXC the count is two single-pumped converters and six double-pumped ones. For the general case, this number can be calculated to be $WK/2$ total single- and double-pumped converters.

V. ROUTING ALGORITHM-CHARACTERIZATION OF BLOCKING

The work of Slepian, Duguid and Hall [27]–[29] has been the basis for proving that the original Benes switch architecture [18], is rearrangeably nonblocking. The famous Slepian and

Duguid theorem considers a three-stage network with $rn \times n$ first and third-stage switches for a total of $N \times N$ inputs and outputs ($N = rn$) as shown in Fig. 14. The theorem states that for the network to be rearrangeably nonblocking, it must have n center-stage switches. The important aspect of this proof is that it is irrelevant how the first and third stages are interconnected with the middle stage as long as full interconnection is guaranteed. It is now instructive to try to explore the rearrangeability properties of the "Twisted Benes" design. Fig. 15 shows an 8×8 "Twisted Benes" design intended for the $2 \times 2/4-\lambda$ WIXC implementation of Fig. 9(a). Subnetworks A, B , and A', B' have been marked on the figure to express the recursive nature of the above proof. The recursive procedure starts from the outermost stages of the network as shown in Fig. 15. In the twisted Benes the outermost stages are connected to the two subnetworks A

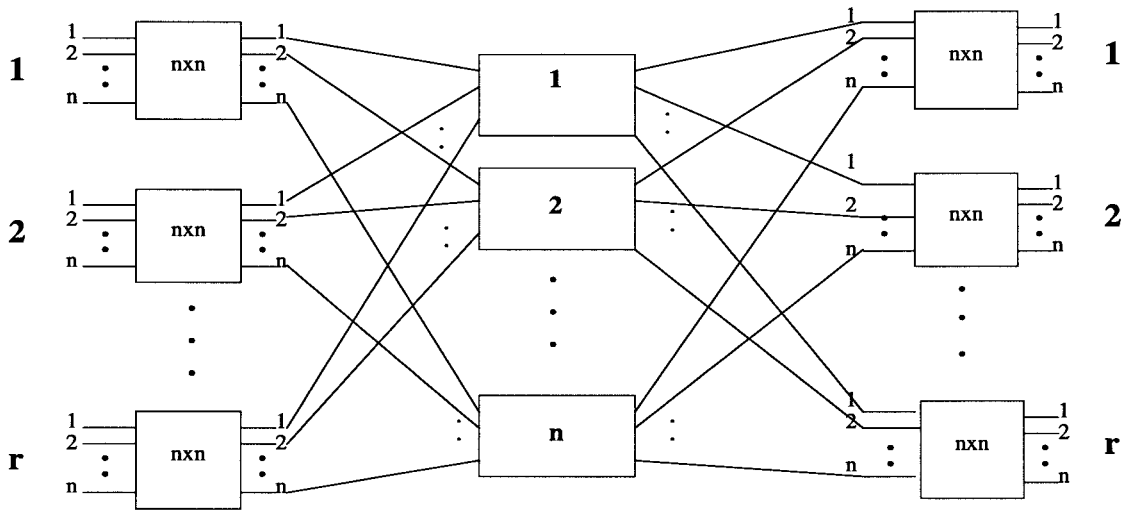


Fig. 14. Proof of rearrangeably nonblocking network based on the Slepian–Duguid theorem.

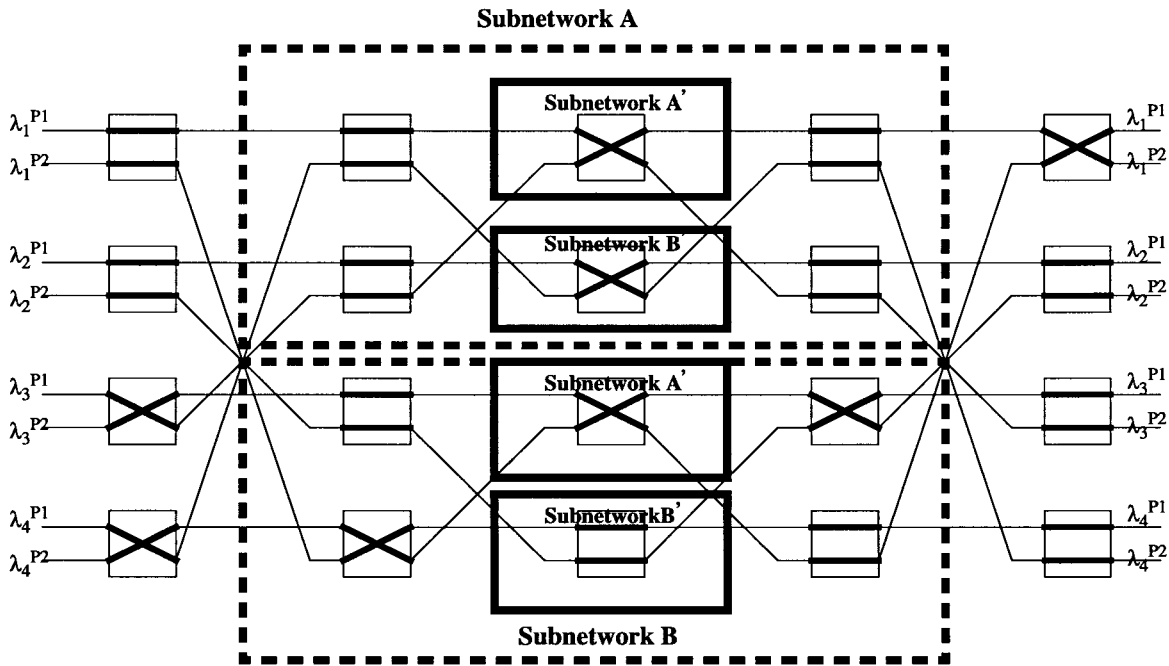


Fig. 15. Use of Slepian and Duguid theorem's recursive nature to prove the "Twisted Benes" design is rearrangeably nonblocking.

and B in a fully connected manner, i.e., each 2×2 in the outmost stages has one input going to each subnetwork A and B . Clearly, the condition required by the Slepian–Duguid theorem has been met so far. Now, we repeat this procedure into each subnetwork A' and B' and observe that again the stage interconnections satisfy Slepian–Duguid requirements. For "Twisted Benes" designs of larger size, recursive proof of the above is straightforward once all subnetworks have been identified. Since the above theorem holds for the "Twisted Benes" design of the paper, we conclude that the design is rearrangeably nonblocking. An immediate result of the above is that there exists a looping algorithm [24] that is used to set-up calls in rearrangeably nonblocking architectures like the original Benes network. The looping algorithm is thoroughly

explained with an example in [30, pp. 87–90]. The looping algorithm can thus be used to set up connections for the "Twisted Benes" design. It has been used to set up the random connections presented in Sections III and IV.

As discussed above, the proposed WIXC architecture is based on the Benes switch fabric that is rearrangeably nonblocking. This essentially means that as connection requests arise, some already existing connections might need to be rearranged in order to accommodate the new ones [30]. This will result in connection interruptions, but no blocking. The proposed WIXC architecture can be easily scaled to become wide-sense nonblocking by adding additional stages and wavelength converters. For the 4×4 Benes, the addition of one extra stage, meaning an additional WSXC and an additional

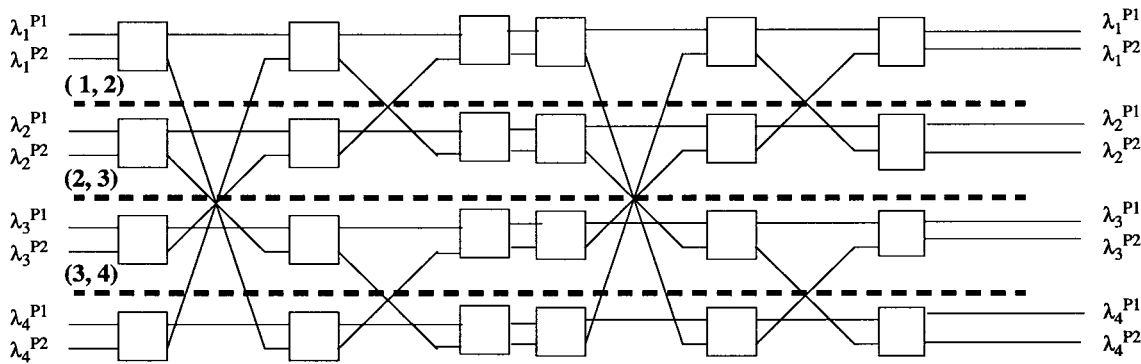


Fig. 16. An 8×8 "Twisted Benes" repetitive design.

DFG converter, makes the switch wide-sense nonblocking [30]. For larger size switches the above is possible by using Cantor networks which are strictly nonblocking space dilations of the Benes fabric but require a very large number of extra components [31]. It is clear that there is a tradeoff between number of components and functionality. In general, utilizing a rearrangeably nonblocking WIXC architecture is beneficial since wavelength conversion is achieved along with space cross-connection with a small number of components. Given a prescribed set of dedicated connections in the network, knowledge of all connections in the list can often be used to accommodate them without conflicts. As a result, connection interruption is likely to occur in assigning a sequence of switched connections rather than a set of dedicated ones, and is further more likely to occur when there is no wavelength conversion rather than when wavelength converters exist. Even with the possibility of connection interruptions, the benefits of the above described architecture far outweigh the benefits of having the strictly nonblocking architecture but with a significantly increased number of WSXC's and all-optical converters. Moreover, the above proposed architecture can be used effectively in cases where partial blocking is allowed (where more input signals than the architecture can handle are present) [32].

VI. COMPONENT ADVANTAGE

One of the most important considerations in choosing a particular WIXC architecture is the number of optical components needed, and in particular the number of wavelength converters. Moreover in our proposed architectures, the number of pumps required for the implementation of the DFG converters (e.g., single-pumped, double-pumped, etc.) becomes important since it was shown that single-pumped DFG converters are preferred, double-pumped DFG converters are allowed but more than two pump waves in a DFG converter cause a number of difficulties. One approach that can be used to construct architectures with simpler DFG wavelength converters (single- and double-pumped only) and potentially to reduce the cost of the resulting WIXC is to use repetitive and modular designs within the WIXC. This facilitates network upgrades in a cost effective manner. Over the years, a variety of multistage interconnection networks were proposed for use

in multiprocessor systems. A significant amount of work was devoted in proving that these networks are indeed rearrangeably nonblocking with the least number of required interconnection stages ($2 \log N - 1$) [35]–[37]. In fact, almost every $(2 \log N - 1)$ -stage network that has been shown to be rearrangeable in the literature is topologically equivalent to the Benes network. Fig. 16 shows an 8×8 "Twisted Benes" design having six stages, each consisting of four 2×2 switching elements. The design has three mirror planes which are noted as dotted lines and are written as: (1, 2), (2, 3), and (3, 4). The design is called a two-pass reverse exchange network [36] since it is essentially a cascade of two copies of a baseline network. The ports of the design of Fig. 16 are labeled so that the network can be converted to the real $2 \times 2/4-\lambda$ architecture of Fig. 17 which includes six four-wavelength 2×2 spatial switches (WSXC's), two single-pumped DFG wavelength converters and two double-pumped DFG wavelength converters. The important aspect of this design is its repetitive nature that makes it potentially low cost. Other repetitive multistage interconnection designs utilizing our "Twisted Benes" architecture are indeed possible but are the subjects of current and future work. For example a topic of current work is a design that will include repetitions of only the first stage of the "Twisted Benes" design shown in Fig. 16 and that will only require single-pumped wavelength converters to achieve $K \times K/W - \lambda$ functionality. Previous work has shown that similar repetitions of a shuffle/exchange network (omega network) followed by its inverse network (reverse omega network) minus one stage produced a rearrangeable network with $2 \log N - 1$ stages [37].

In general, the number of single- and double-pumped DFG converters needed for a $K \times K/W - \lambda$ "Twisted Benes" design is $WK/2$ (Section IV). By comparison, the frequently discussed WIXC architecture of Fig. 2 will require WK single input, single output converters. It is clear that the "Twisted Benes" WIXC architecture provides a significant reduction in the number of wavelength converters needed. The use of repetitive architectures similar to Fig. 16 will provide further cost savings due to its repetitive nature although it might require the same number of components as the "Twisted Benes" or slightly more. As an example, let us consider a $2 \times 2/4-\lambda$ WIXC architecture. Using the repetitive design of Fig. 16 we will need four DFG converters the same as the regular "Twisted Benes"

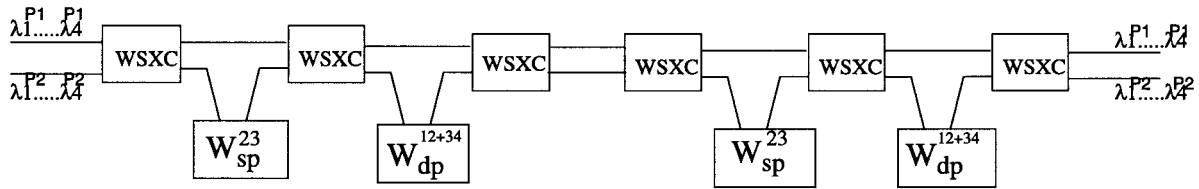


Fig. 17. A $2 \times 2/4-\lambda$ repetitive WIXC actual implementation using DFG parametric wavelength converters.

architecture of Fig. 10. Finally, using the WIXC architecture of Fig. 2 we will need twice as many (8) converters.

VII. CONCLUSION

A wavelength interchange cross-connect architecture that makes use of the DFG wavelength converting device has been presented. This architecture makes use of the unique multichannel wavelength conversion and mirror image mapping properties of the parametric DFG converter. The new architecture is scalable in both the port and wavelength dimensions and there is a systematic way of expanding it to K ports and W wavelengths. The scalable and modular upgradability, the existence of the looping routing algorithm, and a reduction in the number of necessary components make this WIXC architecture particularly attractive.

The above work is obviously not based on a network element that has been built and tested; rather it is a proposal for a new architecture. Since this is a first effort at providing a scalable and transparent WIXC architecture with this type of wavelength converters, significant room for expansion exists in both the architectural as well as the device parts of the work. The performance constraints involved need to be investigated as part of future work. Moreover, the blocking properties of the architecture can certainly improve, although at this point it is not yet clear whether that is essential and if the service disruptions that a rearrangeably nonblocking switch architecture brings can pose a significant restriction in the above networks. The above are subjects of our on-going work.

Although, the feasibility of WIXC's is still under investigation, it is clear that they offer the potential to eventually provide the solution to a "truly" scalable and transparent optical network. They will offer advantages in management and overall network control by providing new network restoration and routing techniques and efficient provisioning and grooming by dividing the networks into more manageable subnetworks.

APPENDIX

As explained in Section II and presented in Fig. 3, a single-pumped DFG converter is easily achieved by putting a wavelength mirror between the appropriate wavelengths. For example, a W_{sp}^{34} represents a single-pumped converter with the wavelength mirror between wavelengths 3 and 4. A double-pumped DFG converter is illustrated in Fig. 18(a), and can be represented as W_{dp}^{12+34} . There are two ways of constructing this converter. Fig. 18(a) presents a DFG converter with two wavelength mirrors between $\lambda_1, \lambda_2, \lambda_3,$ and λ_4 . The use of a bandpass filter will select the desired

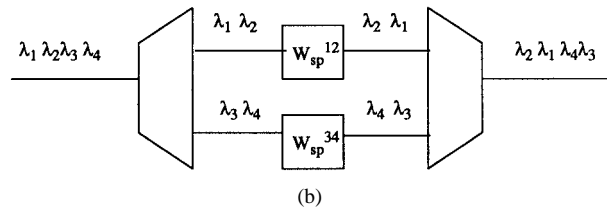
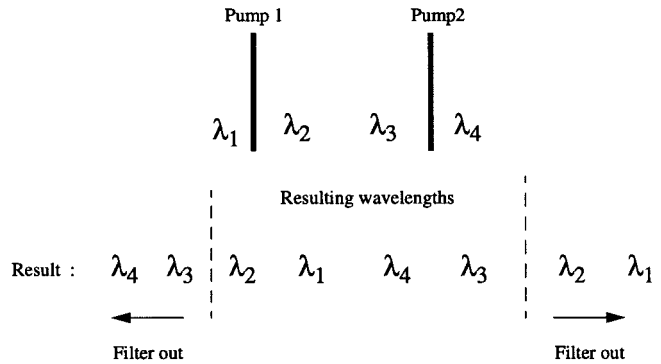


Fig. 18. Implementation of a double-pumped DFG wavelength converter: (a) using two mirror planes and (b) using two single-pumped DFG converters.

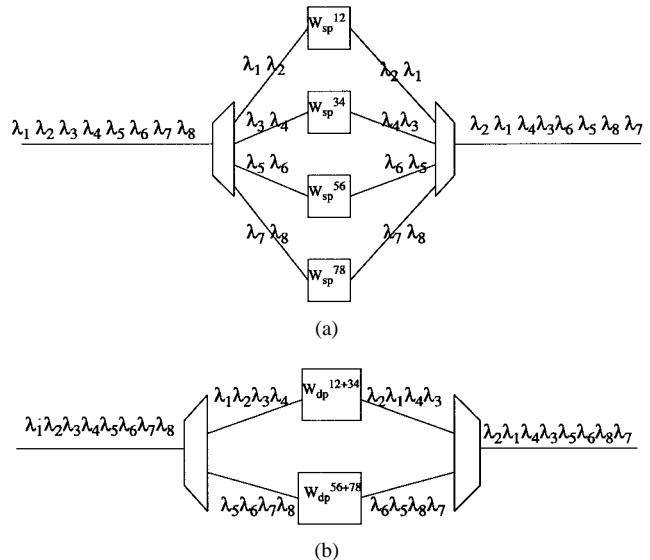


Fig. 19. Implementation of a hybrid converter design to substitute for the nonrealizable quad-pumped DFG converter: (a) using four single-pumped DFG converters and (b) using two double-pumped DFG converters.

converted wavelengths and will filter out the unwanted out-of-band wavelengths as shown. Fig. 18(b) presents an alternative design, where a demultiplexer divides the incoming four wavelengths into two streams carrying respectively two signals

each. These are passed through single-pumped DFG converters with their wavelength mirrors centered between λ_1 , λ_2 , λ_3 , and λ_4 , respectively. As a result the two individual single-pumped converters create the four converted signals which are then multiplexed in a single output stream having the desired frequency arrangements λ_2 , λ_1 , λ_4 , λ_3 . The above multiplexers and demultiplexers can be made using phase-array gratings as described in [33], or multilayer interference filter cascades [34]. As explained in Section IV a quad-pumped DFG converter (W_{qp}) is impractical and will not be considered here. As a result, a hybrid converter, W_{com} which is a combination of single- and double-pumped DFG converters, can achieve wavelength conversion in four wavelength mirror planes. Fig. 19(a) presents the first way of implementing the above, in which a demultiplexer divides the incoming stream of eight wavelengths into four two-wavelength streams. Four single-pumped DFG converters interchange the neighboring wavelength pairs, and a multiplexer recombines them into the stream λ_2 , λ_1 , λ_4 , λ_3 , λ_6 , λ_5 , λ_8 , λ_7 . Another equivalent DFG converter is shown in Fig. 19(b) where a multiplexer divides the incoming wavelength stream into two streams and two double-pumped DFG converters interchange the wavelengths based on the operation principle presented in Fig. 18. The multiplexer then combines these two streams into a single output stream λ_2 , λ_1 , λ_4 , λ_3 , λ_6 , λ_5 , λ_8 , λ_7 .

ACKNOWLEDGMENT

The authors would like to acknowledge the anonymous reviewer for providing insightful comments and valuable correction that initiated further on-going research on the above work. They would also like to thank I. Tomkos for providing useful feedback on this work.

REFERENCES

- [1] M. Fujiwara, M. S. Goodman, M. J. O' Mahony, O. K. Tonguz, and A. E. Willner, "Guest editorial—Multiwavelength optical technology and networks," *J. Lightwave Technol.*, vol. 14, June 1996.
- [2] R. L. Cruz, G. R. Hill, A. L. Kellner, R. Ramaswami, G. H. Sasaki, and Y. Yamabayashi, "Guest Editorial—Optical networks," *IEEE J. Select. Areas Commun.*, vol. 14, June 1996.
- [3] C. A. Brackett, A. S. Acampora, J. Sweitzer, G. Tangonan, M. T. Smith, W. Lennon, K-C. Wang, and R. H. Hobbs, "A scalable multiwavelength multihop optical network: A proposal for research on all-optical networks," *J. Lightwave Technol.*, vol. 11, pp. 736–753, May/June, 1993.
- [4] R. E. Wagner, R. C. Alferness, A. A. M. Saleh, and M. S. Goodman, "MONET: Multiwavelength optical networking," *J. Lightwave Technol.*, vol. 14, pp. 1349–1355, June 1996.
- [5] K. Bala, E. Bouilliet, and G. Ellinas, "The benefits of minimal wavelength interchange in WDM rings," in *Proc. IEEE/OSA Optical Fiber Commun. Conf.*, paper WD2, Dallas, TX, Feb. 1997.
- [6] K. C. Lee and V. O. K. Li, "A wavelength convertible optical network," *J. Lightwave Technol.*, vol. 11, pp. 962–970, May/June, 1993.
- [7] S. Okamoto, A. Watanabe, and K. Sato, "Optical path cross-connect architectures for photonic transport networks," *J. Lightwave Technol.*, vol. 14, pp. 1410–1422, June 1996.
- [8] A. Jourdan, F. Masetti, M. Garnot, G. Soulage, and M. Sotom, "Design and implementation of a fully reconfigurable all-optical cross-connect for high capacity multiwavelength transport networks," *J. Lightwave Technol.*, vol. 14, pp. 1198–1206, June 1996.
- [9] E. Iannone, and R. Sabella, "Optical path technologies: A comparison among different cross-connect architectures," *J. Lightwave Technol.*, vol. 14, pp. 2184–2196, Oct. 1996.
- [10] S. Kuroyanagi and T. Maeda, "An optical cross-connect architecture incorporating failure recovery using reserved wavelengths," in *Proc. Photon. Switching Conf.*, Salt Lake City, UT, vol. 12, Mar. 1995.
- [11] S. J. B. Yoo, C. Caneau, R. Bhat, M. A. Koza, A. Rajhel, and N. Antoniadis, "Wavelength conversion by quasiphase-matched difference frequency generation in AlGaAs waveguides with periodic domain inversion achieved by wafer bonding," *Appl. Phys. Lett.*, vol. 68, no. 19, pp. 2609–2611, May 1996.
- [12] S. J. B. Yoo, M. A. Koza, R. Bhat, and C. Caneau, "Bidirectionally pumped difference frequency generation in AlGaAs waveguides: Polarization-independent, multi-channel wavelength conversion with input signal filtering capabilities," in *Proc. Conf. Lasers Electro-Optics*, San Francisco, CA, May 1998, paper CTUJ4.
- [13] S. J. B. Yoo, "Wavelength conversion technologies for WDM network applications," *J. Lightwave Technol.*, vol. 14, pp. 955–966, June 1996.
- [14] G. P. Agrawal, *Nonlinear Fiber-Optics*. New York: Academic, 1995.
- [15] E. A. Swanson and J. D. Moores, "A fiber frequency shifter with broad bandwidth, high conversion efficiency, pump, and pump ASK cancellation, and rapid tunability for WDM optical networks," *IEEE Photon. Technol. Lett.*, vol. 6, pp. 1341–1344, Nov. 1994.
- [16] G. Hunziker, R. Paiella, D. F. Geraghty, K. J. Vahala, and U. Koren, "Polarization-independent wavelength conversion at 2.5 Gb/s by dual-pump four-wave mixing in a strained semiconductor optical amplifier," *IEEE Phot. Technol. Lett.*, vol. 8, Dec. 1996.
- [17] S. J. B. Yoo, M. A. Koza, C. Caneau, and R. Bhat, "Simultaneous wavelength conversion of 2.5 and 10 Gbit/s signal channels by difference-frequency generation in an AlGaAs waveguide," in *Proc. IEEE/OSA Optical Fiber Commun. Conf.*, San Jose, CA, Feb. 1998, paper WB5.
- [18] V. E. Benes, "On rearrangeable three-stage connecting networks," *Bell Syst. Tech. J.*, vol. XLI, no. 5, Sept. 1962.
- [19] R. A. Thompson and D. K. Hunter, "Elementary photonic switching modules in three divisions," *IEEE J. Select. Areas Commun.*, vol. 14, pp. 362–373, Feb. 1996.
- [20] M. J. Marcus, "Space-time equivalents in connecting networks," in *Proc. Int. Conf. Commun.*, 1970, pp. 35.25–35.31.
- [21] D. A. Smith *et al.*, "Integrated-optic acoustically tunable filters for WDM networks," *IEEE J. Select. Areas Commun.*, vol. 8, pp. 1151–1159, 1990.
- [22] J. Patel, "Liquid crystal and grating-based multiple wavelength cross-connect switch," *IEEE Photon. Technol. Lett.*, vol. 7, pp. 514–516, May 1995.
- [23] M. Z. Iqbal and G. K. Chang, "High performance optical switches for multiwavelength rearrangeable optical networks," in *Proc. Government Microcircuit Application Conf.*, San Diego, CA, Nov. 1994.
- [24] D. C. Opferman and N. T. Tsao-Wu, "On a class of rearrangeable switching networks—Part I: Control algorithms, Part II: Enumeration studies of fault diagnosis," *Bell Syst. Tech. J.*, vol. 50, pp. 1579–1618, 1971.
- [25] G. R. Pieris and G. H. Sasaki, "A linear lightwave Benes network," *IEEE/ACM Trans. Networking*, vol. 1, Aug. 1993.
- [26] N. Antoniadis, K. Bala, S. J. B. Yoo, and G. Ellinas, "A parametric wavelength interchanging cross-connect (WIXC) architecture," *IEEE Photon. Technol. Lett.*, vol. 8, pp. 1382–1384, Oct. 1996.
- [27] A. M. Duguid, "Structural properties of switching networks," Brown Univ., Providence, RI, Progr. Rep. BTL-7, 1959.
- [28] D. Slepian, "Two theorems on a particular crossbar switching network," unpublished manuscript, 1952.
- [29] P. Hall, "On representatives of subsets," *J. London Math. Soc.*, vol. 10, pp. 26–30, 1935.
- [30] H. S. Hinton, *An Introduction to Photonic Switching Fabrics*. New York: Plenum, 1993.
- [31] T. E. Stern and K. Bala, *Multiwavelength Optical Networks: A Layered Approach*. New York: Addison Wesley Longman, Apr. 1999.
- [32] S. J. B. Yoo, "Reduced parametric wavelength-interchanging cross-connect architectures with scalability and modularity," in *Proc. IEEE/OSA Optical Fiber Commun. Conf.*, San Jose, CA, Feb. 1998, paper TuJ3, pp. 59–61.
- [33] M. K. Smit, "Integrated optics in silicon-based aluminum oxide," Ph.D. dissertation, Delft Univ. Technol., Delft, The Netherlands, 1991, ISBN 90-9004261-X.
- [34] M. A. Scobey and D. E. Spock, "Passive DWDM components using microplasma optical interference filters," in *Proc. IEEE/OSA Optical Fiber Commun. Conf.*, San Jose, CA, Feb. 1996.
- [35] A. Varma and C. S. Raghavendra, "Rearrangeability of multistage shuffle/exchange networks," *IEEE Trans. Commun.*, vol. 36, pp. 1138–1147, 1988.
- [36] C.-L. Wu and T.-Y. Feng, "The reverse-exchange interconnection network," *IEEE Trans. Comput.*, vol. C-29, pp. 801–811, Sept. 1980.
- [37] K. Y. Lee, "On the rearrangeability of $(2 \log N - 1)$ -stage permutation networks," *IEEE Trans. Comput.*, vol. C-34, pp. 412–425, May 1985.



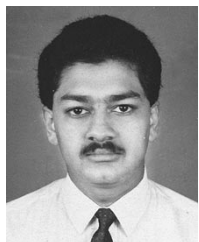
N. Antoniadis (S'93–M'98) received the B.S., M.S., M.Phil., and Ph.D. degrees all in electrical engineering from Columbia University, New York, NY, in 1992, 1993, 1996, and 1998, respectively. His Ph.D. work at Columbia University focused on modeling of optical components, WDM communication systems and networks.

During the period from 1994 to 1998, he participated in research work at Bellcore, Red Bank, NJ, and was involved in both the Optical Networks Technology Consortium (ONTC) as well as the Multi-wavelength Optical Networking (MONET) program. Within MONET, he was a part of a team that designed and developed a wavelength-domain computer simulator for studying performance impairments in WDM optical networks. In 1998, he joined the Photonic Research & Test Center, Corning Inc., Somerset, NJ, where he is currently a Senior Research Scientist doing research on advanced fiber-optic systems and networks to support development of telecommunication fiber and optical network elements. He currently holds one patent in the field of fiber optics.

S. J. B. Yoo (S'82–M'84–SM'97) received the B.S. degree with distinction in electrical engineering, the M.S. degree in electrical engineering, and the Ph.D. degree in electrical engineering with minor in physics, all from Stanford University, Stanford, CA. His Ph.D. dissertation at Stanford University was on linear and nonlinear optical spectroscopy of quantum-well intersubband transitions.

He is an Associate Professor of Electrical and Computer Engineering at University of California (UC), Davis, where his current research involves advanced switching techniques and cross-connects for the Next Generation Internet. Prior to joining UC in 1999, he was a Senior Scientist at Bellcore, Red Bank, NJ, leading technical efforts in optical networking research. His research activities at Bellcore included optical-label switching for the Next-Generation Internet, power transients in reconfigurable optical networks, wavelength interchanging cross-connects, wavelength converters, vertical cavity lasers, and high-speed modulators. He also participated in the ATD/MONET systems integration, the OC-192 SONET Ring studies, and a number of standardization activities. Prior to joining Bellcore in 1991, he conducted research on nonlinear optical processes in quantum wells, four-wave mixing study of relaxation mechanisms in dye molecules, and ultrafast diffusion driven photodetectors. During this period, he also conducted research on life-time measurements of intersubband transitions and on nonlinear optical storage mechanisms at Bell Laboratories and at IBM Research Laboratories, respectively.

Dr. Yoo is a member of the Optical Society of America (OSA) and Tau Beta Pi.



Krishna Bala received the Ph.D. degree in electrical engineering from Columbia University, New York, NY, for his work in routing and wavelength assignment in optical networks.

He is the Manager for Development of Optical Cross-connect products at Tellium, Edison, NJ, and is one of its founders. Before Tellium, he was a Senior Research Scientist at Bellcore responsible for network architecture analysis, where he was the lead network architect for the Multiwavelength Optical Networks project. He has published numerous articles and holds several patents in optical networks. He is the coauthor of a book in this subject.

Dr. Bala received the Bellcore President Excellence award for his work at Bellcore.

Georgios Ellinas (S'93–M'98) received the Ph.D. degree in electrical engineering from Columbia University, New York, NY, in 1998.

Currently, he is a Research Scientist at Telcordia (formerly Bellcore), Red Bank, NJ, working as a member of the Optical Networking Research group. His research interests are in the areas of architectures and control/management of multiwavelength optical networks, fault restoration in mesh optical networks, and packet switching in IP/WDM networks. He is currently participating in the NGI (Next-Generation Internet) project on optical-label switching and the MONET (Multiwavelength Optical Networking) project. From 1993 to 1998, he was a member of the Center for Telecommunications Research at Columbia University conducting research in failure protection in arbitrary mesh networks. Since 1993, he has also been working with the Optical Networking Research program at Bellcore for both the Optical Networks Technology Consortium (ONTC) and MONET projects. He currently holds a position as Adjunct Assistant Professor at Columbia University, teaching a course on Multiwavelength Optical Networking.



Thomas E. Stern (S'54–M'57–SM'67–F'72–LF'95) received the B.S. and M.S. degrees in 1953 and the Sc.D. degree in 1956, all in electrical engineering from the Massachusetts Institute of Technology, Cambridge.

He served in the United States Air Force Research and Development Command from 1956 to 1958, and then joined Columbia University, New York, NY, in 1958. Presently, he holds the Dicker Chair in Electrical Engineering at Columbia University.

He has served in various leadership capacities at Columbia including Chairman of the Department of Electrical Engineering, Technical Director of the Center for Telecommunications Research (CTR), and leader of the CTR's Lightwave Networks Research Group. He holds several patents in communications and has authored two textbooks and over 100 papers in networks and related fields.